

PERIDYNAMIC FRACTURE AND DAMAGE MODELING OF MEMBRANES AND NANOFIBER NETWORKS

F. BOBARU¹, S.A. SILLING², and H. JIANG¹

¹Department of Engineering Mechanics, University of Nebraska-Lincoln, Lincoln, NE 68588-0526, USA

²Department of Computational Physics, Sandia National Laboratories, Albuquerque, NM 87185-0820, USA

ABSTRACT

The peridynamic method used in this paper reformulates the classical continuum mechanics equations by replacing spatial derivatives with an integral of force densities over a region around the material point of interest. This leads to a non-local method that may be thought of as a continuum version of molecular dynamics simulation. Any two material points are connected by a possibly nonlinear, elastic spring (bond) with a critical stretch parameter. We present examples of dynamic fracture and damage for high-aspect ratio structures such as membranes and nanofiber networks. The membrane example captures dynamic transition from a mode III fracture to mode I. In the deformation of nanofiber networks we obtain cellular patterns of deformation when, in addition to the elastic forces along fibers or at bonded contacts between fibers, van der Waals forces are acting between the fibers. The force response across the network is similar to the response observed in rupturing of the protein adhesive in a biological structure (abalone shells).

1 INTRODUCTION

The peridynamic theory (Silling [1]) is based on a reformulation of the classical continuum mechanics equations in which the divergence of stress term is replaced by an integral of the force acting at a material point due to interactions with the rest of the material. This leads to a non-local theory which is fundamentally different from earlier non-local elastic and thermoelastic models (e.g. Eringen and Edelen [2], Eringen [3]) since in the peridynamic formulation no spatial derivatives appear. The consequences of eliminating spatial derivatives are critical in fracture and phase changes problems because, unlike the classical theory, the mathematical structure of the peridynamic theory is unaffected by the emergence of these discontinuities.

In this paper we briefly review the peridynamic formulation and describe several examples of dynamic fracture and damage of materials/structures with very large aspect ratios: thin membranes and networks of fibers and nanofibers.

As suggested by the notion of a continuum version of molecular dynamics, in the peridynamic formulation the acceleration of any particle at x in the reference configuration at time t is found from the equation of motion,

$$\rho \ddot{u}(x, t) = \int_{H_x} f(u(y, t) - u(x, t), y - x) dV_y + b(x, t) \quad (1)$$

where H_x is a neighborhood of x , u is the displacement vector field, b is a prescribed body force density field, ρ is mass density in the reference configuration, and f is a pairwise force function whose value is the force vector (per unit volume squared) that the particle y exerts on the particle x . In the following discussion, we denote the relative position of these two particles in the reference configuration by ξ and their relative displacement by η :

$$\xi = y - x, \quad \eta = u(y, t) - u(x, t) \quad (2)$$

Using these definitions, $\eta + \xi$ represents the current relative position vector between the particles.

The direct physical interaction (which occurs through unspecified means) between the particles at x and y will be called a bond. The bonds extend over a finite distance around a particle; this is a fundamental difference between the peridynamic formulation (PF) and classical continuum mechanics, which is based on the idea of contact forces (interactions between particles that are in direct contact with each other). It is convenient to assume that for a given material there is a positive number δ , called the *horizon*, such that

$$\text{if } |\xi| > \delta \quad \text{then } f(\eta, \xi) = 0 \quad (3)$$

A material is said to be *microelastic* if the pairwise force function is derivable from a scalar *micropotential* w :

$$f(\eta, \xi) = \frac{\partial w}{\partial \eta}(\eta, \xi) \quad \text{for all } \eta, \xi \quad (4)$$

The micropotential is the strain energy in a single bond and has dimensions of energy per unit volume squared. The energy per unit volume in the body at a given point (i.e., the local strain energy density) is therefore found by integrating the strain energy in all bonds between the given point and surrounding material points within the horizon (see e.g. Silling [1], Silling and Bobaru [4]).

If a body is composed of a microelastic material, work done on it by external forces is stored in recoverable form in much the way as in the classical theory of elasticity. Furthermore, it can be shown that the micropotential depends on the relative displacement vector η only through the scalar distance between the deformed points and thus,

$$\hat{w}(p, \xi) = w(\eta, \xi) \quad p = |\eta + \xi| \quad (5)$$

For isotropic materials, the relationship in (5) can be further written as

$$\tilde{w}(p, q) = \hat{w}(p, \xi) \quad q = |\xi| \quad (6)$$

Bonds with linear elastic behavior can be modeled using a quadratic micropotential $w(p, \xi) = c(\lambda - 1)^2 g(q)$. Here c is a positive constant and $\lambda = p/q$ is the bond stretch. The function g defines whether bonds with different reference lengths can have different elastic response. In practice, g has little effect except with regard to deformations that occur on a length scale smaller than the horizon. For example, the wave dispersion properties of the material at small wavelengths are affected by terms of this type (see Silling [1]). A prototype for a non-linear elastic behavior that leads, in the case of a homogeneous deformation of a membrane, to a macroscopic strain energy equal to that of a classical Blatz-Ko rubbery material, is obtained when we take $w(p, q) = c(\lambda^2 + 1/\lambda^2 - 2)g(q)$ (Silling and Bobaru [4]).

For nanostructured materials, such as nanofiber networks, long-range forces like van der Waals forces may play an important role in the mechanics of deformation of such structures. The peridynamic formulation allows inclusion of such forces in a natural way. In addition to the micropotential above, we consider a Lennard-Jones (LJ) type potential that acts between any two material points. To avoid having to model each individual atom as in molecular dynamic simulations, we choose to use the elastic interactions (peridynamic forces) between material points along an individual fiber and augment that with van der Waals forces acting between fibers. Points of contact between two fibers may or may not have microelastic bonds. Van der Waals interactions will always be present between nodes on any two different fibers as long as the nodes are in the action range of this force. The range of action of the long-range forces (van der Waals) does not have to be the same as the horizon of the peridynamic forces. The total potential we use in this case is

$$\tilde{w}(p, q) = w_{el}(p, q) + w_{LJ}(p), \quad w_{LJ}(p) = \alpha \left(\frac{a}{p} \right)^{12} - \beta \left(\frac{a}{p} \right)^6 \quad (7)$$

where the LJ potential depends only on the relative distance in the current configuration, $p = |\eta + \xi|$.

2 DAMAGE AND FRACTURE IN THE PERIDYNAMIC FORMULATION

Damage may be incorporated into a peridynamic constitutive model by allowing the bonds for solid interactions to break irreversibly (e.g. Silling and Bobaru [4], Silling and Askari [5]). The simplest assumption is that this breakage occurs when a bond is extended beyond some predetermined critical bond deformed length. Since the breakage is irreversible, time and position must now be included as arguments in the interparticle force, for example

$$\hat{f}(p, q, x, t) = f(p, \xi) \mu(\xi, x, t) \quad (8)$$

where μ is a history-dependent function defined by:

$$\mu(\xi, x, t) = \begin{cases} 1, & \text{if } p < p_0 \quad \text{for all } 0 \leq \tau \leq t \\ 0, & \text{otherwise} \end{cases} \quad (9)$$

with p_0 being the critical value of bond deformed length for breakage. (p_0 may depend on reference bond length q .) Recall that any particle in the continuum has an infinite number of bonds connecting it to other particles. During deformation, some of these bonds may break as determined by eqns (8)-(9), and breakage of the bonds occurs independently among different bond lengths and orientations for a given particle. In practice, bond breakage in a peridynamic body usually evolves in such a way as to form two-dimensional surfaces. These surfaces correspond to cracks; their growth is the way fracture propagation occurs spontaneously in the peridynamic theory. The initiation and growth process occurs without reference to any supplemental kinetic relation that controls crack growth on the basis of a stress intensity factor or similar quantity. In this sense, fracture modeling in the peridynamic theory is “autonomous” and represents a fundamental difference between the present theory and the techniques of traditional fracture mechanics. Long-range forces, such as van der Waals forces, are not subject to damage.

3 NUMERICAL EXAMPLES

This section presents some examples of predictions of membrane and nanofiber network deformation and failure according to the theory discussed above. Because it is based on integral equations, which are less amenable to exact solutions than PDEs in initial value problems, all of the present results were obtained using a numerical solution method. The numerical method itself is described elsewhere (Silling and Askari [5], Silling [6]).

3.1 Tearing of a membrane

In this example, a rectangular membrane is held fixed along three sides. The fourth side is free, except for a segment that is pulled upward (out of the plane) and forward (toward the interior of the membrane) with constant velocity. The membrane has a density of 1200kg/m^3 and a thickness of 0.5mm . It is modeled as a brittle microelastic material with a bulk modulus of 300MPa and a critical stretch to failure $\lambda_0 = 0.1$.

Stress concentrations are created at the ends of the segment that is lifted. These stress concentrations eventually nucleate cracks that propagate into the rectangle. The two cracks, when they are nucleated, are mostly in mode III, but as they advance they become mostly mode I. This mode transition occurs because, as the cracks move away from the boundary, the membrane can more easily displace and rotate out of the plane in such away that the loading near the crack tips becomes tensile. This loading is such that the cracks tend to advance toward each other and eventually intersect, forming a more or less triangular fragment that completely separates from the rectangular membrane.

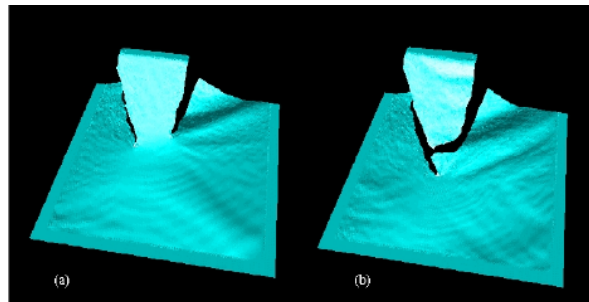


Figure 1. Tearing of a rectangular membrane. Transition from mode III to mode I fracture.

Figure 1 shows the predicted result just before the two cracks merge and the triangular section separates. Because of the asymmetry of the boundary condition (the prescribed velocity segment is

closer to one rigid boundary than the other), the cracks grow at different speeds and curve as they grow. As the problem progresses, the slower of the cracks starts to be influenced strongly by the free surface created by the faster crack, and it turns sharply toward this free surface. This tendency of initially parallel cracks in a membrane to merge as they advance is familiar to anyone who has unwrapped a packaged CD or a candy bar. It is also of technological interest in predicting damage to thin structures, such as aerospace structures as a result of impact.

3.2 Large deformation of a random network of nanofibers

Membrane-like networks of electrospun polymer continuous fibers of nanometer scale diameters have been recently produced in the laboratory (e.g. Dzenis [7], Li and Xia [8]). It is of importance to analyze the mechanical behavior of such networks built from randomly oriented fibers or from aligned fibers. In the examples below we use a linear model for the peridynamic bond elasticity with a maximum stretch of 30% (at which point the bond breaks) and maximum compression of 10% (at which point contact repulsive forces prevent interpenetration of material). The micromodulus is chosen to correspond to a Young's macro modulus of 1.5 GPa. The fibers interact through peridynamic forces, as well as through long-range forces (van der Waals forces). The latter are used only between nodes belonging to different fibers. These interactions influence the deformed shape of the network, which includes cellular patterns, as shown below. Fibers that are close enough or in contact with one another are considered bonded through peridynamic (solid-like bonds).

The constants in the LJ potential (7) we use in these examples are $\alpha=\beta=1.1$ and $a=1\text{nm}$. This makes the van der Waals force repulsive for a separation distance less than about 1nm, while the peak (attractive) force is obtained around 1.4 nm. The force decreases to 10% of its peak value for a separation distance of 2nm. A convergence study is performed to determine the necessary spacing between the discretization nodes in fibers such that the total van der Waals force between parallel adjacent fibers is insensitive to the exact locations of the nodes.. In figure 2 we show two such configurations for fibers of length 200nm. The distance between the two fibers is 1.5nm.

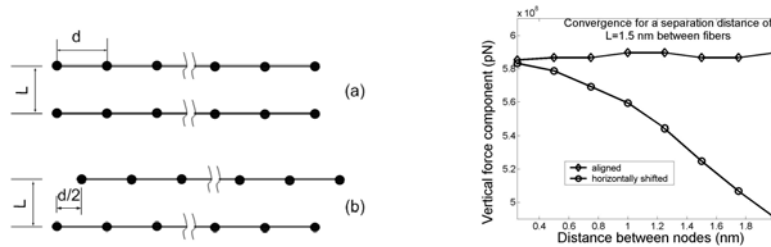


Figure 2. Two configurations, aligned (a) and horizontally shifted (b), for determining the necessary grid for converged long-range forces. On the left, the variation of the total van der Waals force between the two fibers in the two selected configurations versus the spacing between the discretization nodes. For a spacing of 1nm the relative error is less than 3%.

The spacing between nodes varies from 0.2nm to 2nm. For sufficiently dense nodes along each fiber, the vertical component of the total force exerted by one fiber on the other should be, roughly, the same. The plot in figure 2 shows that a distance of 1nm between the nodes the dependence of the total force on the different, but practically equivalent, configurations becomes less than 3%. In the examples that follow we use this separation distance between the nodes along each fiber.

We generate 3D curves with preferred orientation inside a parallelepiped box (400nm by 400nm by 5nm) as described in Bobaru and Silling [9]. The fibers are then rotated with randomly chosen angles from a uniform distribution. The fiber network geometry mimics that of real nanofiber networks obtained using the electrospinning process (see Dzenis [7], Li and Xia [8]). The network is clamped at

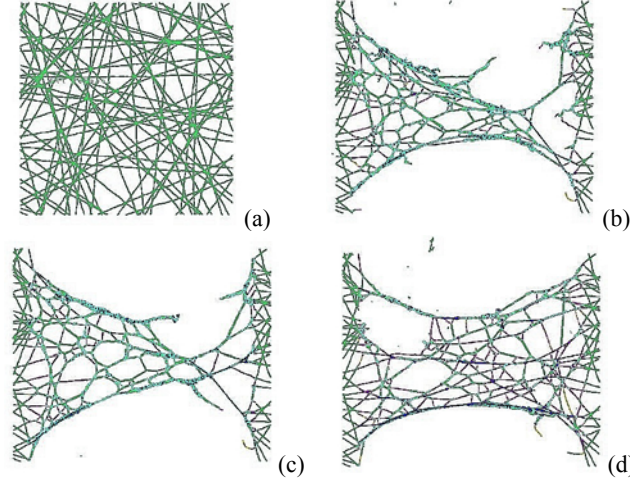


Figure 3. The undeformed configuration (a). The deformed shape of the network after 14 ns (b-d). In (b) all qualified crossovers are bonded by peridynamic bonds (case 1). In (c) only 30% of crossovers are bonded and the critical stretch of bonds between fibers is obtained from a Gaussian distribution of mean 1 (the critical stretch along a fiber) and standard deviation of 0.1 (case 2). In (d) the standard deviation is 0.9 (case 3).

the left and right ends and the length of the network becomes 360nm. We conduct the following numerical simulations:

1. *Fully crosslinked, constant linkage strength.* All crossovers are bonded (solid-like bonds). The critical stretch of the bonds between the fibers is the same as that of bonds within a fiber.
2. *Partially crosslinked, low variability in linkage strength.* Only 30% of the crossovers are bonded. These bonded crossovers are randomly selected from the total number of crossovers. The critical stretch of the bonded crossovers is varied such that its distribution follows a normal random distribution with mean equal to the critical stretch of bonds within a fiber and standard deviation equal to 10% of the mean value (the mean value is 1 and the standard deviation we select is 0.1).
3. *Partially crosslinked, high variability in linkage strength.* Same as case 2, but the standard deviation is 0.9 compared to the mean value of 1. We use the same “map” of connected bonds as in case 2, but the critical stretches associated with pairs of nodes will differ from case 2. Some of the bonded crossovers break at much lower stretches than that for bonds along a fiber, while others break at stretches larger than that of bonds along a fiber. We call the “weaker” bonds “sacrificial bonds”.

The left and right ends of the network are moved away from one another with constant velocity of 3nm/ns. The initial velocity profile along the network varies linearly from one end to the other. We follow the deformation and damage of the network until total failure. In figure 3 we show the undeformed and deformed configurations for the three cases. The total force in the direction of motion across the vertical midplane that right half of the network is exerting on the left half is plotted versus time in figure 4. We observe that the peak force increases from case 1, to case 2, and case 3. That is due to the fact that there are some bonds between fibers that have a larger critical stretch than the constant value of the critical stretch for the bonds within each fiber. Moreover, with the larger population of weaker crossovers in cases 2 and 3, the network is able to rearrange itself more easily and provide better strength in doing so. This is illustrated in figure 4, in which the saw-tooth behavior of the load in case 3 is most pronounced since here is where we have the largest number of sacrificial bonds at the crossovers between fibers. The sacrificial bonds are broken, the network rearranges, and a second force peak is reached. Case 3 also has increased toughness, as well as increased peak load,

because the additional sawtooth peaks in figure 4 add to the area under the load-stretch curve, which is a measure of the work required to fail the network.

The predicted enhancement in overall network toughness due to variability in crossover strength appears to have a precedent in biology. We note the similarity between the configuration with sacrificial bonds and experimental results observed when a natural polymer adhesive binding the microstructure of abalone shell is subjected to stretch in an AFM (see Smith et al [10]). In this work it was found that the adhesive fibers elongate in a stepwise manner as folded domains or loops are pulled open. The elongation events occur for forces of a few hundred piconewtons, which are smaller than the forces of over a nanonewton required to break the polymer backbone in the threads. Smith et al [10] indicate that this “modular” elongation mechanism might prove to be responsible for the extreme fracture toughness of the abalone shell.

4 CONCLUSIONS

The peridynamic model, because it incorporates damage and failure as a natural aspect of deformation, does not require a pre-existing defect to initiate crack growth. It therefore may offer a means to analyze the deformation and failure of nearly perfect materials such as may occur at the nanoscale. At the macroscale, the theory also offers the advantage of “autonomous” crack modeling, in which supplemental relations that control crack evolution are not necessary. For example, there is no need for a relation that governs crack growth speed or direction in terms of a stress intensity factor. The crack growth is determined instead as a consequence of the equation of motion and constitutive model.

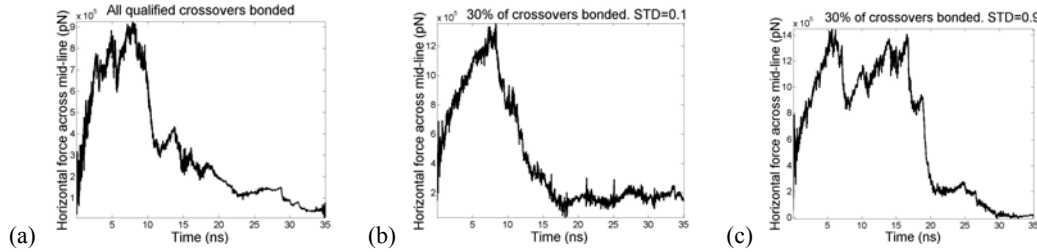


Figure 4. Force versus time for the cases described in figure 3. Notice that the peak force increases from (a) to (b) to (c). Also, the saw-tooth appearance in (c), where we have a significant number of sacrificial bonds (case 3), is similar to the response of natural polymer adhesive in ultra-tough abalone shells (e.g. Smith et al [10]).

Therefore this approach may allow for arbitrarily complex patterns of growth among multiple, mutually interacting cracks.

A peridynamic model for fracture in a membrane is capable of capturing the transition from a mode III crack to a mode I crack. Peridynamic models of nanofiber networks allow easy consideration of long-range forces (such as van der Waals forces) without having to model individual atoms. Our analysis of nanofiber networks shows promise in numerically modeling and designing nano-structured materials with extreme properties that can replicate the extraordinary fracture toughness resistance of some biological materials, such as that of the abalone shells (e.g. Smith et al [10]).

ACKNOWLEDGMENTS

Sandia is a multiprogram laboratory operated by Sandia Corporation, a Lockheed Martin Company, for the United States Department of Energy's National Nuclear Security Administration under contract DE-AC04-94AL85000.

5 REFERENCES

- [1] Silling SA, Reformulation of elasticity theory for discontinuities and long-range forces, *Journal of the Mechanics and Physics of Solids*, 48, 175–209 (2000).
- [2] Eringen AC, Edelen DGB. On non-local elasticity. *International Journal for Engineering Science* 10, 233-248 (1972).
- [3] Eringen AC. Theory of Nonlocal elasticity and some applications. *Res Mechanica* 21, 313-342 (1987).
- [4] Silling SA, Bobaru F. Peridynamic modeling of membranes and fibers. *International Journal of Non-Linear Mechanics* 40(2-3), 395-409 (2005).
- [5] Silling SA, Askari E. Fracture Modeling With a Meshfree Peridynamic Method. *Computers and Structures* – under review (2004).
- [6] Silling SA, Dynamic fracture modeling with a meshfree peridynamic code, in *Computational Fluid and Solid Mechanics 2003*, K.J. Bathe (ed.), Amsterdam, Elsevier Science, 641–644 (2003).
- [7] Dzenis Y. Spinning continuous fibers for nanotechnology. *Science* 304 (5679): 1917-1919 (2004).
- [8] Li D, Xia Y. Electrospinning of Nanofibers: Reinventing the wheel? *Advanced Materials* 16(14), 1151-1170 (2004).
- [9] Bobaru F, Silling SA. Peridynamic 3D models of nanofiber networks and carbon nanotube-reinforced composites, in *Materials Processing and Design: Modeling, Simulation and Applications, NUMIFORM 2004*, S. Ghosh, J.C. Castro, and J.K. Lee (eds), American Institute of Physics, 1565-1570 (2004).
- [10] Smith BL, Schaffer TE, Viani M, et al. Molecular mechanistic origin of the toughness of natural adhesives, fibres and composites. *Nature* 399 (6738): 761-763 (1999).